Catena 242 (2024) 108083

Contents lists available at ScienceDirect

Catena

journal homepage: www.elsevier.com/locate/catena

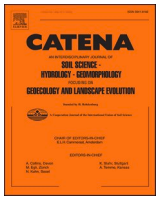

Variations in provenance and transport of terrestrial organic matter in the Changjiang River during the flood season

Yameng Wang [a], Chenglong Wang [a,c,*], Chuchu Zhang [a], Qihang Liao [a,b], Ziyue Feng [a,d], Xinqing Zou [a,b,*]

[a] School of Geography and Ocean Science, Ministry of Education Key Laboratory for Coast and Island Development, Nanjing University, Nanjing 210023, China
[b] Collaborative Innovation Center of South China Sea Studies, Nanjing University, Nanjing 210093, China
[c] Changjiang River Scientific Research Institute, Wuhan 430010, China
[d] Guangzhou Marine Geological Survey, Guangzhou 511458, China

ARTICLE INFO

Keywords:
Particulate organic carbon
Biomarker
Human activities
Changjiang River

ABSTRACT

River is a crucial channel for the transport of terrestrial organic carbon (OC_{terr}) into the sea, and has significant implications for the global carbon cycle. However, with the intensification of human activities within the watershed (such as dams and changes in land use), the sediment and OC_{terr} output from rivers have significantly decreased. To study the influence of human activities on the provenance and transport of particulate organic carbon (POC) exported from the Changjiang River Basin (CRB), we collected suspended particulate matter samples during the rainy season of 2021. The POC content exhibited an increasing trend from the headwater zone to the estuary. Results of three-end-member mixing model indicated that both soil-derived and autochthonous OC (OC_{auto}) contributed approximately more than 40.0 %. Notably, OC_{auto} experienced a significant increase from the Three Gorges Dam (TGD) to estuary in the mainstem, attributed to the sediment interception effect of the TGD. The POC contents in the headwater zone and Jinshajiang River in 2021 were lower compared to those in 2007, which can be attributed to a decrease in cultivated land area and increase sediment trapping by cascade dams. Affected by TGD, the POC content in the middle and lower reaches as well as the delta zone first decreased in 2003 and then increased from 2007 to 2021. Additionally, the degradation of lignin phenols and *n*-alkanes was influenced by the TGD, which prolonged the retention time of terrestrial plants. Compared to previous studies, the decrease in soil-derived OC and increase in OC_{auto} in CRB, influenced by dams and land use, could have long-lasting effect on carbon burial in the ECS.

1. Introduction

Rivers play an important role for the transport of terrestrial organic carbon (OC_{terr}) to the ocean. OC_{terr} and its properties within the rivers reflect both natural and human processes within the drainage basin (Galy et al., 2015). The OC_{terr} is often divided into dissolved organic carbon (DOC) and particulate organic carbon (POC). During transport, a portion of POC decomposes and re-enters the atmosphere in the form of CO_2 (Fearnside and Pueyo, 2012), while the remaining portion is buried in sediment (Galy et al., 2007, 2008). Globally, 200 Mt y^{-1} of POC is transported by rivers to the ocean (Galy et al., 2015), with a significant portion coming from the large rivers in Asia, accounting for approximately 40 % of the POC transported from land to ocean (Galy et al., 2008; Park et al., 2018). The Changjiang River (CJR) is the longest and largest river in Asia (with the largest water discharge and drainage basin area), annually transporting 122 Mt of sediment to the East China Sea (ECS) (CWRCMWR, 2016–2021), carrying a substantial amount of OC_{terr}. The exported POC from the CJR is deposited in the estuary and transported southward, playing a crucial role in OC exchange between land and oceans.

The POC in rivers were mainly from biospheric OC (terrestrial plants, aquatic in-situ primary producers, and pre-aged soil) and petrogenic OC (Galy et al., 2015; Hilton, 2017). The unstable nature of POC varies depending on its sources. Since algae-derived POC is more easily degraded than terrestrial plants- and soil-derived OC due to its labile OC composition, such as amino acids, carbohydrates, and lipids (Mannino

* Corresponding authors at: School of Geography and Ocean Science, Ministry of Education Key Laboratory for Coast and Island Development, Nanjing University, Nanjing 210023, China.
E-mail addresses: clwang@nju.edu.cn (C. Wang), zouxq@nju.edu.cn (X. Zou).

https://doi.org/10.1016/j.catena.2024.108083
Received 31 January 2024; Received in revised form 14 April 2024; Accepted 3 May 2024
Available online 8 May 2024

and Harvey, 1999; Canuel and Hardison, 2016). Therefore, the composition of POC will affect its fate during transportation.

The intensification of human activities within the watershed, such as reservoirs, land use, and water and sediment regulation, has altered the sources and transport of POC in global rivers. The numerous dams on the upper reaches of the Godavari River are increasing the in-situ production of organic carbon, while limiting the transport of organic carbon upstream (Kirkels et al., 2022). Besides, organic carbon in the Red River system was mainly derived from erosion and soil leaching in the basin (Le at al., 2017). Large lakes, reservoirs, and navigable ponds upstream of the Upper Mississippi River Basin increased more productive downstream reaches (Voss et al., 2017), while POC were likely derived primarily from terrestrial C_3 plants in the Lower reach (Cai et al., 2015). Water-Sediment Regulation Scheme influenced the source of POC in the lower Yellow River (Hu et al., 2015). Moreover, most studies in the Changjiang River Basin were conducted before 2010, indicating that soil organic matter was the dominant source of the POC in the rainy season of 1997, 2003, 2006, 2009, and 2010 (Wu et al., 2007b; Yu et al., 2011; Wang et al., 2012; Wu et al., 2018), with some contribution from terrestrial plant debris (Wu et al., 2018). However, there is a lack of quantitative analysis on the contribution of POC sources during the rainy season in the Changjiang River basin (CRB). The soil-derived OC was dominant in the mainstem CJR, with proportions of 37 %-49 % and 44 %-56 % in 2009 and 2010, respectively (Wu et al., 2018). While, the autochthonous POC (OC_{auto}), derived from in-situ primary producers (including phytoplankton, aquatic vascular plants, benthic algae, and mosses, Peterson et al., 1985; Onstad et al., 2000), was often overlooked (Wu et al., 2007b; Wu et al., 2018). After the construction of the Three Gorges Dam (TGD), there was a significant decrease in the absolute supply of POC flux to the lower reaches of the CJR and the ECS between 2003 and 2006 (Yu et al., 2011). The particulate terrestrial OC transported by the Changjiang River in 2006 decreased to less than two-thirds of that in 2003 (Yu et al., 2011; Wang et al., 2020a). Especially, the TGD intercepted 82 % of the sediments from the upper reach of the CJR annually between 2016 and 2021 (CWRCMWR, 2016–2021). Moreover, the CRB has undergone extensive human activities in recent years (Yang et al., 2015). The completion of the Jinshajiang River cascade dams resulted in the significant interception of sediment from the headwater zone (Yang et al., 2018; Wang et al., 2022b), leading to an 80–88 % decrease in POC transported in the Jinshajiang River from 2003 to 2012 to 2013–2019 (Wang et al., 2022b). Furthermore, the implementation of a ten-year protection policy for the CRB since 2016 has resulted in substantial changes in land use, including a 5 % increase in cultivated land area and a 37 % reduction in soil erosion from 1990 to 2020 (CWRCMWR, 2005, 2006-2015, 2018, 2020). As a result of above-mentioned activities, there has been an increase in OC_{auto} flux export from the CJR (Wang et al., 2022b; Zhao et al., 2022). Despite increasing attention to local OC_{auto}, there is still limited research on the quantitative sources of POC in the CRB, especially after 2016. Therefore, it is necessary to conduct a quantitative analysis of the POC sources to elucidate the changes under the influence of human activities.

The objectives of this study were to: i) determine the sources of POC in the CRB during the flooding season; ii) investigate the spatiotemporal variations in the sources, transport, and degradation of POC in the CRB during the flooding season; iii) explore the relationship between land use, soil erosion, dam construction, and the sources of POC in the CRB during the flooding season. In order to reveal changes in POC content and sources, the sampling results during the flood season in previous studies were compared.

2. Materials and methods

2.1. Study area

The CJR is globally renowned as the third longest river and the fourth largest in terms of fluvial sediment load (Jiang et al., 2013). CRB exhibits a warm climate and experiences abundant rainfall. The CJR carried 70 % of water and 86 % of sediment load during the flood season (May–October), which transported 70 % of the POC flux every year (Wang et al., 2011a; CWRCMWR, 2016–2021). Therefore, sampling in the flood season can well represent the overall characteristics of suspended POC transport. And CRB has a multi-level and stepped terrain, flowing through mountains, plateaus, basins (tributaries), hills, and plains (Fig. 1c). Therefore, CRB is rich in hydropower resources. The construction of over 50,000 dams, including the TGD, has significantly reduced sediment discharge into the ECS, decreasing from 413 Mt yr^{-1} prior to 2003 (Wang et al., 2011b) to 118 Mt yr^{-1} between 2016 and 2021 (CWRCMWR, 2016–2021). Especially, sediment from the headwater zone and Jinshajiang River has been considerably reduced due to the trapping effect of cascade dams since 2012 (Yang et al., 2018). Given the pronounced spatial variation within the CRB concerning landscape, rock type, land use, climate, and precipitation, we have divided the region into five distinct parts (Fig. 1a): the headwater zone (from the TTR to BT), Jinshajiang River reach (from BT to YB), upper reach (from YB to YC), the middle and lower reaches (from YC to DT), and the delta zone (from DT to XLJ). This division follows the standard established by Guo et al. (2019). The tributaries of the CJR are distributed across the headwater zone (BQ and CME River), the upper reach (Yalongjiang, Minjiang, Jialingjiang, and Wujiang River basins), the middle and lower reaches (Hanjiang River, Dongting Lake, and Poyang Lake basin), and the delta zone (Tai Lake basin). The vegetation cover along the river is diverse and abundant (Yu et al., 2007), reflecting a heterogeneous pattern of various land use types (Guo et al., 2015). According to the Chinese Multi-period Land Use Cover Change dataset, the areas of cultivated land, woodland, grassland, water body, construction land, and unused land in the CRB in 2020 were 47.7×10^4 km^2 (26.8 %), 73.4×10^4 km^2 (41.3 %), 41.0×10^4 km^2 (23.1 %), 5.6×10^4 km^2 (3.1 %), 5.3×10^4 km^2 (3.0 %), 4.8×10^4 km^2 (2.7 %), respectively. In addition, the middle and lower reaches of the CJR (1.7×10^5 km^2) and its tributaries (7.3×10^4 km^2) have the largest area of cultivated land, while the woodland (9.6×10^4 km^2) and grassland (6.9×10^4 km^2) of Jinshajiang River reach were relatively prosperous. The developed land was concentrated in the middle and lower reaches of the CJR and the delta zone (total area of mainstem and tributaries 4.1×10^4 km^2; Table S3, Supplementary Material).

2.2. Sample collection

During the rainy season of 2021, a total of 47 surface water samples were collected along the entire CRB. These samples encompassed 20 samples from the mainstem and 27 samples from various tributaries (Fig. 1a). More than 200 L of surface water at each sampling site was stored in clean polyethylene buckets directly pumping from a depth of 0.3 m horizontally in the middle of the river from a bridge or boat in time series. To obtain the suspended particulate matter for analysis, water samples were filtered using pre-combusted (450℃, 4 h) Whatman GF/F filters with a pore size of 0.7 μm 1 L each time within three hours after collection. According to the concentration of suspended particulate matter, multiple filters can be used at a sampling point until all water samples have been filtered. The filters were carefully preserved at a temperature of −20℃ and subsequently subject to freeze-drying using a vacuum freeze drier. The dried samples were ground using an agate mortar.

2.3. Laboratory analysis

After homogenization, the samples were acidified using 4 mol/L HCl and decalcified for 24 h. Subsequently, the materials were thoroughly rinsed with deionized water and dried in an oven at a temperature of 55 °C. For the determination of the POC and stable isotope ($\delta^{13}C$) contents, a Thermo Flash 2000 elemental analyzer interfaced with a MAT-253 isotope ratio mass spectrometer was utilized. The precision of the

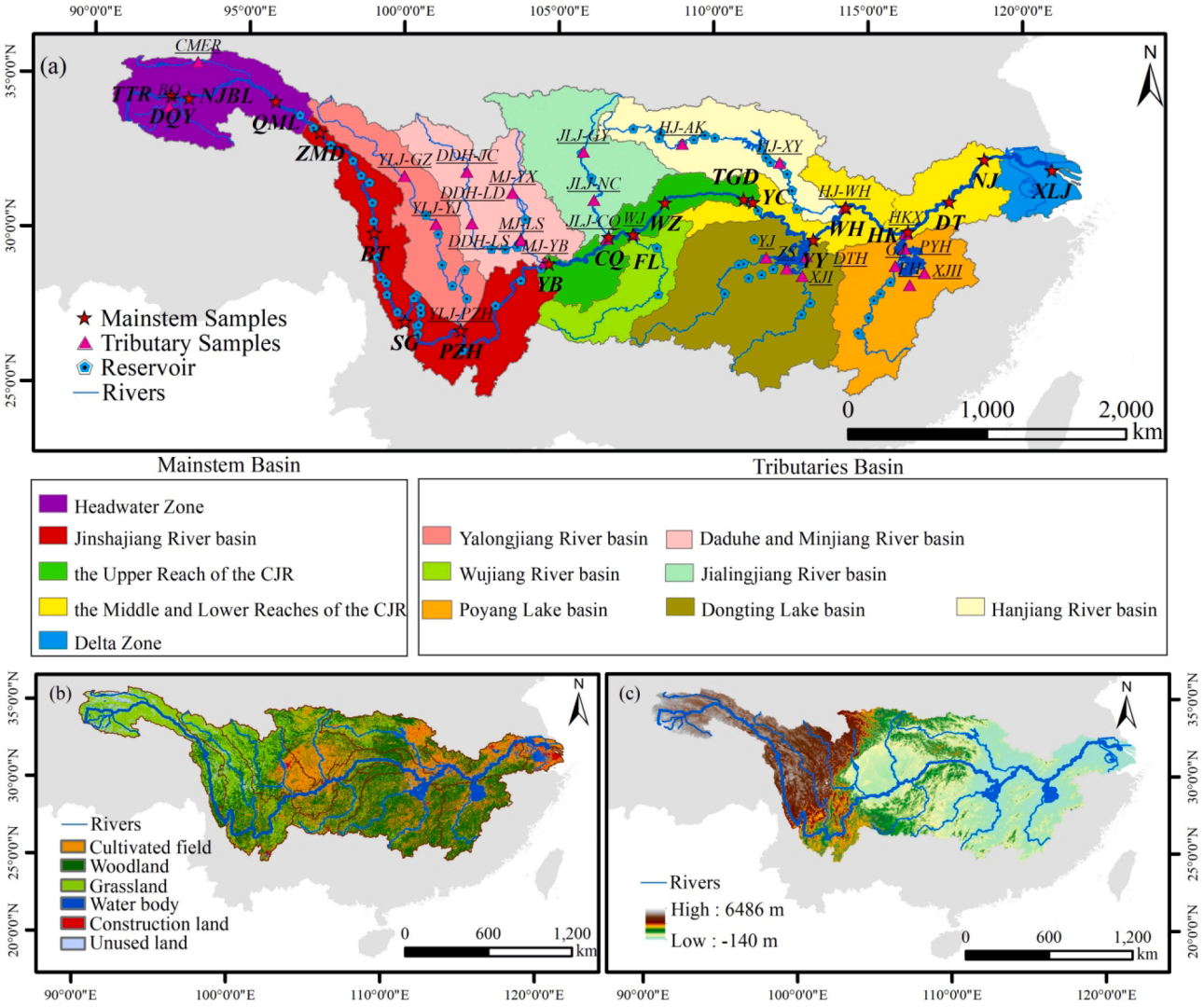

Fig. 1. (a) Samples collected from CRB. Pentagrams represent the mainstem samples and triangles indicate tributaries samples. The detailed information of sampling points for the mainstem and tributaries of CJR were shown in Table S1 and S2, Supplementary Material. (b) Land use type of the CRB. The data was taken from Xu et al. (2023). (c) Elevation of the CRB.

POC determination was better than ± 0.02 ‰. The precision of the $\delta^{13}C$ was better than ± 0.1 ‰, using standard notation relative to the VPDB (Vienna Pee Dee Belemnite) standard. Further details regarding the methodology can be found in Xing et al. (2011).

The analysis of lignin phenols followed the CuO oxidation method as described by Yu et al. (2011). In brief, 1.0 g of dried and homogenized sample was digested with 1.0 g CuO and 0.05 g $Fe(NH_4)_2(SO_4)_2$ in 15 mL 2 M NaOH under vacuum conditions at a temperature of 170 °C for a duration of 3 h. Following cooling to room temperature, recovery standards including ethyl vanillin (EV) and *trans*-cinnamic acid (CA) were added. The pH of the mixture was adjusted to 1 using HCl, after which the mixture was extracted three times with ethyl acetate and subsequently dried using a nitrogen blow-dry method. The reaction products were converted to trimethylsilyl derivatives using bis(trimethylsilyl)trifluoroacetamide (BSTFA, 99 %)/trimethylchlorosilane (TMCS, 1 %). The analysis of lignin phenols was performed using a Thermo Fisher 1300 gas chromatograph (GC) equipped with a flame ionization detector.

5 G of dry homogeneous sample was combined to 15 mL solution of dichloromethane-methanol (DCM:MeOH = 1:1) in polytetrafluoroethylene (PTFE) teflon tubing. The suspension was vigorously vortexed for 30 s, followed by a 15-minute sonication period. This extraction process was repeated for four times, and the resulting supernatants were combined. The mixture was then concentrated to 0.5 mL and blow dry with nitrogen gas. Then a solution of 2 mL KOH-MeOH was added for saponification at a temperature of 40 °C for 12 h. The extraction of neutral lipids was carried out using 2 mL of hexane each time, resulting in four extraction cycles. The concentrated solution was then passed through a chromatography column containing 10 mL of *n*-hexane. The *n*-alkane compounds were determined using a GC (Thermo 1300) instrument. The GC analysis procedure for the *n*-alkanes involved the following steps: The temperature was initially raised from 80 °C (held for 2 min) to 140 °C at rate of 10 °C/min, and then further increased to 315 °C (held for 25 min) at rate of 4 °C/min

2.4. Calculation of n-alkanes

n-alkane compounds are valuable tracers commonly used as to identify sources of OC due to their specific resistance to degradation and distinctive source characteristics. Short-chain *n*-alkanes (n-C_{15}, n-C_{17}, and n-C_{19} widely exhibit a unimodal distribution) are primarily derived from aquatic algae and bacteria (Meyers, 1997; Meyers, 2003; He et al., 2020). Mid-chain *n*-alkanes, represented by n-C_{21}, n-C_{23}, and n-C_{25} with a maximal unimodal distribution, are commonly associated with

macrophytes, both emergent and submerged (Ogura et al., 1990; Meyers, 2003; He et al., 2020). By contrast, long-chain *n*-alkanes (*n*-C_{27}, *n*-C_{29}, and *n*-C_{31}) are widely utilized as indicators of terrestrial plants (Bourbonniere and Meyers, 1996; Meyers, 1997; Meyers, 2003; Rao et al., 2014).

The Carbon Preference Index (CPI) is a parameter that reflects the relative abundance of odd and even carbon *n*-alkanes. A CPI value greater than 1 indicates a dominance of odd carbon atoms within the calculated carbon number range, while a CPI value less than 1 suggests a dominance of even carbon atoms within the calculated carbon number range. Generally, *n*-alkanes derived from higher plants exhibit a clear odd-carbon dominance (Wu et al., 2001). The CPI value is also employed to indicate the degradation state of *n*-alkanes (Fahl and Stein, 1997; Yamamoto et al., 2008). The CPI value in living plants typically exceeds 5 and gradually decreases to 1 as degradation progresses (Rieley et al., 1991). To facilitate a more comprehensive analysis of the *n*-alkane, short-chains ($CPI_{14\text{-}22}$) and long-chains ($CPI_{25\text{-}33}$) were analyzed separately. The calculation formula for CPI is as follows:

$$CPI_{14-22} = 0.5 \times \left[\sum (C_{15} + C_{17} + C_{19} + C_{21})/(C_{14} + C_{16} + C_{18} + C_{20}) + \sum (C_{15} + C_{17} + C_{19} + C_{21})/(C_{16} + C_{18} + C_{20} + C_{22}) \right] \quad (1)$$

$$CPI_{25-33} = 0.5 \times \left[\sum (C_{25} + C_{27} + C_{29} + C_{31} + C_{33})/(C_{24} + C_{26} + C_{28} + C_{30} + C_{32}) + \sum (C_{25} + C_{27} + C_{29} + C_{31} + C_{33})/(C_{26} + C_{28} + C_{30} + C_{32} + C_{34}) \right] \quad (2)$$

2.5. Calculation of lignin phenols

The lignin phenol concentration was expressed as Σ8 (mg 10 g^{-1} dry weight), including cinnamyl phenols (p-coumaric and ferulic acid), syringyl phenols (syringaldehyde, acetosyringone, and syringic acid), and vanillyl phenols (vanillin, acetovanillone, and vanillic acid). Λ8 (mg 100 mg TOC^{-1}) is the Σ8 normalized to 100 mg of organic carbon. The ratios of syringyl/vanillyl (S/V) and cinnamyl/vanillyl (C/V) can provide insights into the plant sources and degradation status of POC. A C/V ratio of less than 0.05 indicates woody tissue, while a C/V ratio greater than 0.2 suggests non-woody tissue (Hedges and Mann, 1979). While, S/V ratio is close to 0 in gymnosperms and higher than 0.4 in angiosperms (Hedges and Mann, 1979). Furthermore, the ratios of acid to aldehyde of vanillyl phenols (Ad/Al)v from fresh plants are generally lower than 0.4 (Hedges et al., 1988; Goñi et al., 1993).

2.6. Three-end-member mixing model

To determine the relative contributions of different OC sources in the CRB, a three-end-member mixing model was utilized. This model incorporated the values of OC to organic nitrogen (C/N) ratio and $\delta^{13}C$ to estimate the fractional contributions of the soil (f_s), terrestrial plants (f_{tp}), and autochthonous OC (f_{au}) to the POC source in the CJR.

$$C/N = [f_s \times C/N_s] + [f_{tp} \times C/N_{tp}] + [f_{au} \times C/N_{au}] \quad (3)$$

$$\delta^{13}C = [f_s \times \delta^{13}C_s] + [f_{tp} \times \delta^{13}C_{tp}] + [f_{au} \times \delta^{13}C_{au}] \quad (4)$$

$$f_s + f_{tp} + f_{au} = 1 \quad (5)$$

Owing to sediment trapping by the TGD, the impact of sediments from the upper reach on the middle and lower reaches was reduced (Yu et al., 2011). The end-member values above and below sample point YC were different. In addition, previous studies have shown that C_3 plants were dominant in the CRB (Yu et al., 2007), so the C/N ratio and $\delta^{13}C$ of C_3 plants were uniformly used in the model for terrestrial plants. Please refer to Table 1 for further detail. To account for the variability in end-member values, a random sampling Monte Carlo simulation strategy was employed using MATLAB (version R2021b, MathWorks, USA). This simulation approach, as described by Andersson (2011), allowed for the assessment of source variability in the end-member values.

2.7. Statistical analyses

Pearson's correlation analysis was employed to assess the significance of the relationships between the environmental parameters and biomarker distributions. To conduct these analyses, SPSS software (version 21.0, BM, SPSS, USA) was used for all analyses.

3. Results

3.1. Bulk properties in the CRB

Fig. 2 illustrates the values of POC content, $\delta^{13}C$, and C/N ratio of suspended particulate matter in CRB. The POC content in the mainstem CJR increased from the headwater zone to the estuary (Fig. 2a), ranging from 0.20 % to 2.04 % (an average of 0.87 % ± 0.55 %, n = 20). In comparison, the POC contents in the tributaries that converge into the middle and lower reaches were higher than that in the tributaries that converge into the upper reach and headwater zone (Fig. 2b). The $\delta^{13}C$ values were in the range of − 26.99 ‰ and − 23.74 ‰ in the mainstem (mean value of − 25.18 ‰ ± 0.82 ‰), and gradually become negative along CJR (Fig. 2c), indicating an increase in OC_{auto}. Similarly, $\delta^{13}C$ values in the middle and lower reaches were relatively low compared to the values in upper reach and headwater zone in tributaries (Fig. 2d). The mean value of C/N ratio in the mainstem (8.22 ± 0.90, Fig. 2e) was greater than that in the tributaries (7.66 ± 1.49, Fig. 2f)). Specifically, in tributaries, values of C/N ratio greater than 10 occurred in the Yalongjiang River, Daduhe River, and Minjiang River, suggesting the contribution from soil OC.

3.2. Lignin phenols in the CRB

The parameters of lignin phenols were determined to analyze the contribution from terrestrial plants (Fig. 3a-j). Overall, Λ8 and Σ8 values show relatively consistent trend in the mainstem (Fig. 3a and c), gradually decreasing along the CJR. And it might be consistent with the vegetation coverage area (Fig. 1b and Table S3, Supplementary Material). The Λ8 and Σ8 values in Jialingjiang River showed an increasing

Table 1
The end-member values of C/N ratio and $\delta^{13}C$ from soil, terrestrial plants, and OC_{auto}, as indicated by mean ± standard deviation.

End element	Sample points above YC		Sample points below YC		References
	C/N ratio	$\delta^{13}C$/‰	C/N ratio	$\delta^{13}C$/‰	
Soil	9.7 ± 3[a]	− 23.0 ± 2[b]	9.7 ± 3[a]	− 23.0 ± 2[b]	Guo, 2015; Wu et al., 2018;
Terrestrial plants	25.3 ± 9.9[c]	− 31.7 ± 2[d]	25.3 ± 9.9[c]	− 28.5 ± 2[d]	Yu et al., 2007; Wu et al., 2018; Sun et al., 2021
OC_{auto}	6.0 ± 2.0[e]	− 30.0 ± 2.6[e]	6.0 ± 2.0 [e]	− 30.0 ± 2.6[e]	Wei et al., 2020

[a] The C/N ratio values of soil is from Guo (2015).
[b] The $\delta^{13}C$ values of soil is from Wu et al. (2018).
[c] The C/N ratio value of terrestrial plants is from Sun et al. (2021).
[d] The $\delta^{13}C$ ratio value of terrestrial plants is from Yu et al. (2007) and Wu et al. (2018).
[e] The C/N ratio and $\delta^{13}C$ ratio value of OCauto is from Wei et al. (2020).

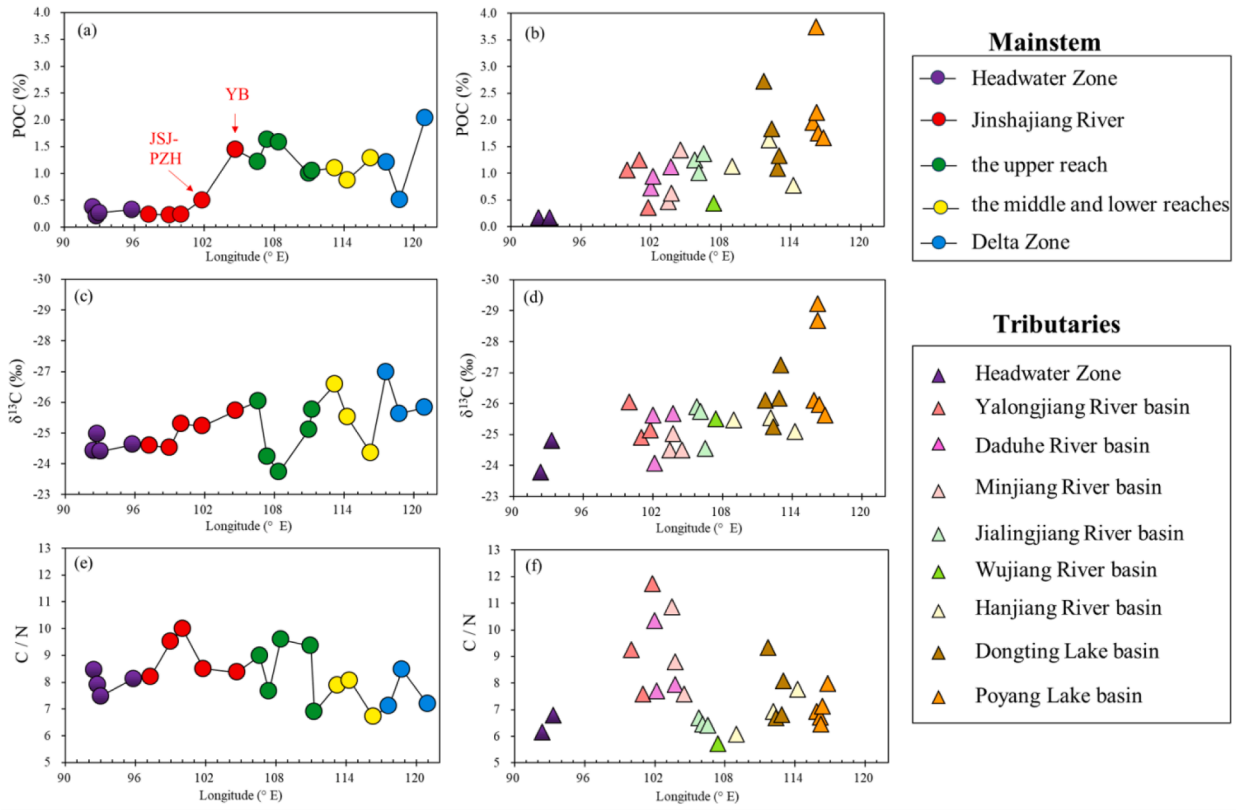

Fig. 2. Spatial distribution of bulk OC properties of suspended particles in mainstem and tributaries of the CRB. (a, b) POC content, (c, d) $\delta^{13}C$ value, (e, f) C/ N ratio.

trend from upstream to downstream, while the values were low in the middle reaches and high in the upstream and downstream of the Yalongjiang River, Daduhe River, Minjiang River, and Hanjiang River (Fig. 3b and d). The C/V and S/V ratios fluctuated and increased from the headwater zone to the estuary (Fig. 3e and g), reflecting changes from woody to non-woody and from gymnosperms to angiosperms. However, in tributaries, the C/V and S/V ratios were higher in the middle and lower reach (suggesting non-woody angiosperms, Fig. 3f and h) than in the Jinshajiang River basin (woody gymnosperms, Fig. 3f and h) and the upper reach (woody angiosperms, Fig. 3f and h). The (Ad/Al) v values decreased along runoff in the CRB (Fig. 3i and j), implying a decrease in the degree of lignin phenols degradation.

3.3. *n*-alkanes in the CRB

At most sampling points, the *n*-alkanes ranged from *n*-C_{14} to *n*-C_{35}. The concentrations of *n*-alkanes varied from 456.0 ug g TOC^{-1} to 7153.6 ug g TOC^{-1} in the mainstem (Table 2) and from 604.2 ug g TOC^{-1} to 10909.2 ug g TOC^{-1} in the tributaries (Table 3). Specifically, the concentrations of short-chain (*n*-C_{15}, *n*-C_{17} and *n*-C_{19}) and long-chain *n*-alkanes (*n*-C_{27}, *n*-C_{29} and *n*-C_{31}) were high in both mainstem and tributaries (Table 2 and 3). While, the mid-chain (*n*-C_{21}, *n*-C_{23} and *n*-C_{25}) contents were only accounted for about 10 % of the total *n*-alkanes concentrations, showing the fewer OC from macrophytes. The $CPI_{14\text{-}22}$ values rose along the CJR and suggested the decrease in the degree of degradation of short-chain *n*-alkanes. However, the improving $CPI_{25\text{-}33}$ indicated the increase in the degree of degradation of long-chain *n*-alkanes.

3.4. Sources of POC in the CRB

C/N ratio, $\delta^{13}C$, lignin phenols, and *n*-alkanes serve as indicators of different sources of POC in the CRB and can complement each other. Typically, terrestrial soil and plants have a high C/N value, while aquatic phytoplankton has a low C/N value (Meyers, 1997). Additionally, shifts in $\delta^{13}C$ during diagenesis can indicate the selective loss of specific fractions of OC with different compositions (Onstad et al., 2000). Most of the sampling points in both the mainstem and tributaries fell within the range close to soil and phytoplankton (Fig. 4), highlighting the significance of contributions from soil-derived OC and autochthonous OC. Lignin phenols and *n*-alkanes can indicate the source of terrestrial plants, and *n*-alkanes can also reflect OC from phytoplankton. The three end-member mixing model is an effective tool for quantitatively analyzing POC sources. And the results were presented in Fig. 5. The POC in the CRB was primarily composed of soil-derived OC and OC_{auto} (Fig. 5a, b, e and f), which aligned with the dominance of short- and mid-chain *n*-alkanes observed in the CRB (Table 2 and 3). In the mainstem, the mean contribution of soil-derived OC (50.3 % ± 5.4 %) was slightly higher than the value of OC_{auto} (37.8 % ± 5.1 %), while the terrestrial plants proportion was the lowest (11.9 % ± 1.4 %) (Fig. 5a, c and e). The proportions of OC from tributary soil (47.0 % ± 7.3 %), in-situ primary production (41.3 % ± 7.4 %), and terrestrial plants (11.8 % ± 2.4 %) were similar to those from the mainstem (Fig. 5b, d and f).

4. Discussion

4.1. Characteristics and influencing factors of POC transport in the CRB

The distribution of POC in the CRB exhibited certain patterns along the river, with variations observed in different sections. The POC content generally increased from the headwater zone to the estuary (Fig. 2a), while the $\delta^{13}C$ decreased along the river in both the mainstem and the tributaries (Fig. 2b). The C/N ratios decreased from the upper reach CJR to estuary (Fig. 2c). Notably, there was a significant and sharp increase in POC content by approximately twice from JSJ-PZH to YB. The contributions from tributaries such as the Minjiang River and Daduhe River cannot be overlooked, as they have relatively large C/N

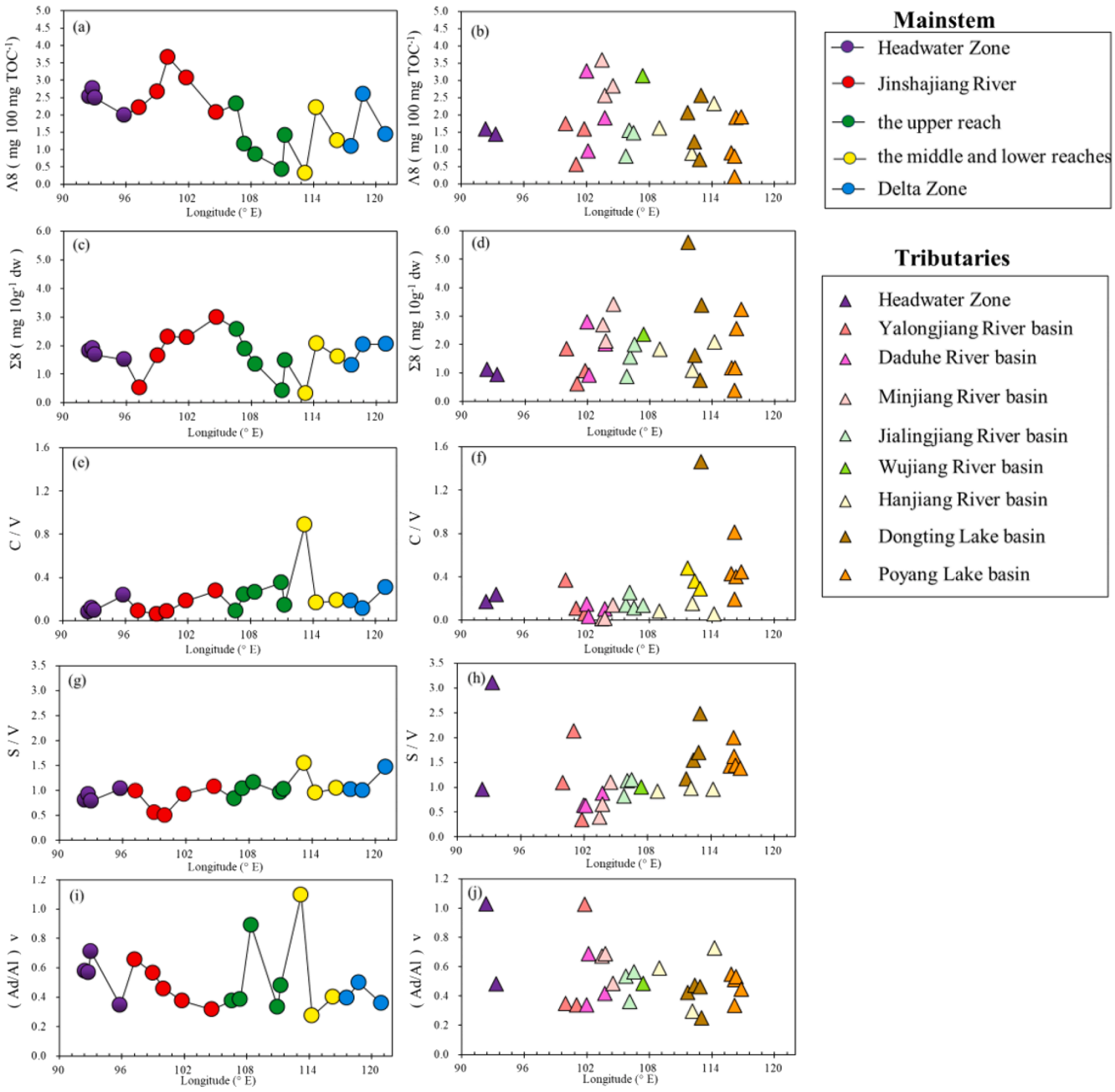

Fig. 3. Spatial distribution of lignin phenols parameters in the mainstem and tributaries of the CRB. (a, b) Λ8 contents, (c, d) Σ8 contents, (e, f) C/ V ratio, (g, h) S / V, and (i, j) (Ad/Al)v.

ratios and $\delta^{13}C$ values (Kendall et al., 2001; Wu et al., 2007a). The POC content at JSJ-PZH and YB were 0.50 and 1.44, respectively, while it was 0.35 at YLJ-PZH and 1.43 at MJ-YB (Fig. 2a). This indicated the significant contribution from Minjiang River. It can be seen that the content of POC decreased notably from upstream to downstream of the Yalongjiang River (Fig. 2a), primarily due to the presence of several cascade dams, particularly between YLJ-YJ and YLJ-PZH (Fig. 1a), which intercepted a substantial amount of suspended sediment (Wang et al., 2020b). Similarly, the Hanjiang River, also featuring numerous cascade dams, displayed a downward trend. Generally speaking, after dam construction, there will be a large amount of suspended particulate matter deposition, and algae proliferation in the reservoir, which will increase the POC content. However, research has found that the density of algae in the Yalongjiang River, Han River, and Minjiang River during the 2020 rainy season was relatively low compared to other areas in the Changjiang River Basin (Hu et al., 2022). Therefore, it may not be possible to provide sufficient OC_{auto}. However, in the case of the Daduhe River and Minjiang River, the POC content increased from upstream to downstream, with only one dam situated between MJ-YX and MJ-LS (Fig. 1a), where the capture effect of dams on sediment might be not significant. Furthermore, the C/N ratios in the mainstem exceeded the inflow value of the Jialingjiang River, Daduhe River, Minjiang River, and Wujiang River, indicating that these tributaries had a significant impact on the C/N ratio of the mainstem of the CJR.

The Λ8 values show a decreasing trend from the headwater zone to the estuary in the CRB (Fig. 3a), while the degree of degradation did not show an increase (Fig. 3e), indicating a reduced contribution of lignin to POC along the river course. The $\delta^{13}C$ values gradually became negative along the runoff (Fig. 2b), indicating that the contribution of soil organic carbon is far inferior to that of terrestrial plants. On the other hand, long-

Table 2
Concentrations of *n*-alkanes and selected parameters in mainstem of the CRB.

River reaches	Sampling sites	Longitude (°E)	Latitude (°N)	*n*-C_{14-35} /ug g TOC^{-1}	*n*-C_{15} + *n*-C_{17} + *n*-C_{19} /ug g TOC^{-1}	*n*-C_{21} + *n*-C_{23} + *n*-C_{25} / ug g TOC^{-1}	*n*-C_{27} + *n*-C_{29} + *n*-C_{31} / ug g TOC^{-1}	CPI_{14-22}	CPI_{25-33}
Headwater Zone	TTR	92.44	34.22	1268.9	23.5	111.8	737.0	0.86	8.27
	DQY	92.77	34.03	3995.2	337.9	536.2	1716.0	0.73	5.65
	NJBL	93.02	34.13	1617.5	18.3	99.7	1019.8	0.72	7.80
	QML	95.82	34.02	3389.2	1020.8	327.7	400.9	1.37	1.36
Jinshajiang River	ZMD	97.25	33.01	4281.3	230.8	482.9	1979.0	0.58	4.42
	BT	99.01	29.77	7153.6	1971.8	837.0	2068.1	2.23	4.50
	SG	100.01	26.89	6746.2	1623.0	1003.6	1646.5	1.40	4.81
	PZH	101.81	26.60	3606.1	818.9	353.4	1151.8	1.87	3.99
	YB	104.67	28.77	961.5	95.9	99.6	382.1	1.02	4.46
Upper Reach of CJR	CQ	106.61	29.62	1289.5	250.3	109.1	437.6	1.75	3.63
	FL	107.39	29.71	1009.4	130.6	88.7	344.5	1.16	3.57
	WZ	108.42	30.74	1632.5	169.7	229.2	234.1	1.00	1.13
	TGR	110.97	30.86	1302.5	363.5	131.2	92.5	1.07	0.85
	YC	111.27	30.76	1538.7	301.7	101.4	394.7	1.04	2.35
Middle and Lower Reaches of CJR	YY	113.23	29.54	1066.9	271.8	96.0	81.5	0.95	0.77
	WH	114.29	30.57	1634.7	457.2	129.7	466.9	2.02	3.58
	HK	116.30	29.80	456.0	54.6	39.0	127.9	0.74	3.20
	DT	117.63	30.77	1155.3	173.0	104.4	361.9	1.27	2.27
	NJ	118.77	32.13	1104.0	147.5	122.3	303.8	1.13	2.29
Delta Zone	XLJ	120.96	31.79	1051.0	51.0	23.6	400.9	2.61	1.29

Table 3
Concentrations of *n*-alkanes and selected parameters in tributaries of the CRB.

River reaches	Sampling sites	Longitude (°E)	Latitude (°N)	*n*-C_{14-35} /ug g TOC^{-1}	*n*-C_{15} + *n*-C_{17} + *n*-C_{19} /ug g TOC^{-1}	*n*-C_{21} + *n*-C_{23} + *n*-C_{25} / ug g TOC^{-1}	*n*-C_{27} + *n*-C_{29} + *n*-C_{31} / ug g TOC^{-1}	CPI_{14-22}	CPI_{25-33}
Headwater Zone	BQ	92.37	33.86	4442.1	309.6	574.4	2219.0	1.40	5.24
	CMER	93.31	35.31	10909.2	4416.7	1241.8	611.0	2.57	0.67
Jinshajiang River	YLJ-GZ	99.99	31.61	1997.7	100.4	362.5	993.5	1.42	5.84
	YLJ-YJ	101.01	30.04	957.5	230.0	88.0	123.0	1.20	0.87
	YLJ-PZH	101.80	26.61	3067.3	899.4	468.5	502.6	2.14	2.10
	DDH-JC	102.01	31.74	2689.7	419.4	503.3	1057.8	2.07	6.61
	DDH-LD	102.17	30.07	1399.9	140.8	203.9	545.1	0.97	4.02
	DDH-LS	103.75	29.56	2025.7	458.7	234.1	647.3	2.18	3.80
	MJ-YX	103.48	31.05	1250.2	313.7	87.6	429.3	2.29	3.97
	MJ-LS	103.76	29.53	1304.5	429.7	94.0	336.6	2.06	3.37
	MJ-YB	104.53	28.82	604.2	159.8	42.5	191.0	2.57	5.25
Upper Reach of CJR	JLJ-GY	105.78	32.39	1439.4	393.2	159.2	100.4	1.08	0.83
	JLJ-NC	106.12	30.82	1241.2	149.5	100.2	483.7	1.15	4.56
	JLJ-CQ	106.54	29.56	1179.7	164.4	61.6	444.8	0.94	4.50
	WJ	107.41	29.71	2226.7	376.5	163.9	765.2	1.38	3.63
Middle and Lower Reaches of CJR	YJ	111.70	28.96	632.4	99.2	39.5	212.3	1.01	3.25
	ZS	112.37	28.61	1490.1	119.4	54.6	723.0	1.22	4.74
	XJ I	112.87	28.36	1166.4	284.7	123.5	129.0	1.26	0.87
	DTH	113.00	29.00	803.1	71.5	66.9	352.3	1.10	3.25
	HJ-AK	108.98	32.65	1365.5	219.4	88.2	490.4	1.26	3.40
	HJ-XY	112.14	32.03	1201.0	17.2	51.9	920.5	2.98	7.09
	HJ-WH	114.24	30.58	1833.4	455.5	186.1	480.7	2.23	2.38
	GJ	115.88	28.69	2220.5	693.4	186.3	445.8	1.61	2.51
	PYH	116.19	29.25	1037.9	186.8	49.8	244.8	0.65	2.48
	HKX	116.21	29.74	1202.8	164.8	37.3	617.3	3.18	3.49
	FH	116.34	28.07	888.8	247.1	65.3	283.8	3.40	3.78
	XJ II	116.82	28.46	1784.8	228.7	164.2	726.0	1.64	3.46

chain *n*-alkanes decreased from the headwater zone to the TGD. The observations were consistent with the analysis of land use types in the CRB, where the area of woodland and grassland decreases from the headwater zone to the estuary (from 1.0 × 10^5 km^2 to 0.5 × 10^5 km^2, Fig. 1b and Table S3, Supplementary Material). This decrease in vegetated areas may impact the input of terrestrial plant-derived POC into the river. In addition, we observed a decrease in Λ8 values accompanied by relatively high (Ad/Al)v in the Jinshajiang River and upper reach of

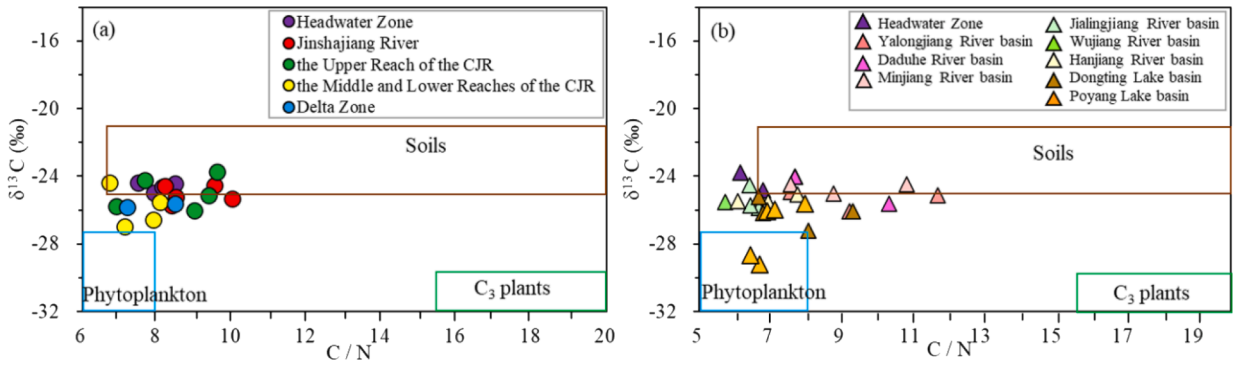

Fig. 4. C/N ratio and $\delta^{13}C$ of POC in the mainstem (a) and tributaries (b) of the CRB. The isotopic and elemental compositions of different end-members are taken from Yu et al. (2007), Guo (2015), Wu et al. (2018), Wei et al. (2020), and Sun et al. (2021).

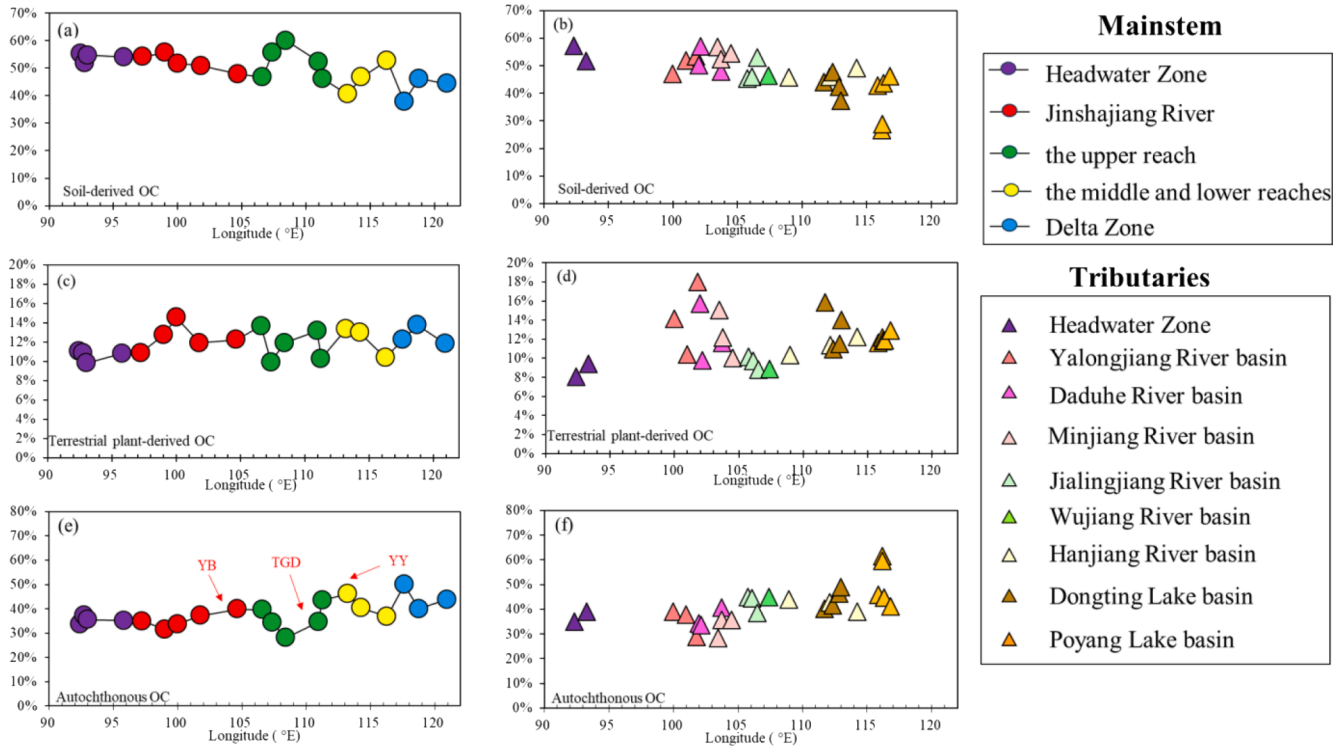

Fig. 5. Three-end-member mixing model results for proportions of soil (a, b), terrestrial plants (c, d), and OC_{auto} (e, f) in mainstem and tributaries of the CRB.

the CJR, which may be related to the interception of sediment by cascade dams and TGD. The C/V and S/V values increase from the headwater zone to the estuary (Fig. S1a and 1b, Supplementary Material). This trend is particularly evident in the middle and lower reaches CJR, including Dongting Lake and Poyang Lake, where the C/V and S/V values are significantly higher compared to the upper reach CJR (Fig. S1b, Supplementary Material). This suggests that the contribution of non-woody angiosperms, rather than woody gymnosperms, becomes more prominent in the middle and lower reaches.The (Ad/Al)v ratios were mostly greater than 0.4, especially in the tributaries where the values are higher than in the mainstem. This suggests that OC derived from terrestrial vegetation has undergone microbial degradation. The decreasing contribution of lignin phenols to POC corresponds to the decrease in terrestrial vegetation coverage across the CRB.

The contents of total *n*-alkanes were higher at the sample sites in the headwater zone and Jinshajiang River compared to the upper reach CJR and downstream areas (Table 2). Both short- and long-chain *n*-alkanes were more abundant than mid-chain *n*-alkanes in most samples from the mainstem. Short-chain *n*-alkanes exhibited an increasing trend from the headwater zone to the TGD station, indicating the significant contribution of phytoplankton productivity of POC. Moreover, the tributaries with dam constructions, such as the Yalongjiang River, Daduhe River, Minjiang River, and Hanjiang River, showed an increase in short-chain *n*-alkanes along the river (Table 3). This can be attributed to the increased transparency resulting from dam interception, which promotes the prosperity of phytoplankton in the river (Tian et al., 2021). The $CPI_{14\text{-}22}$ ranged from 0.5 to 3.5, indicating a lower degradation level compared to the $CPI_{25\text{-}33}$, which varied from 0.5 to 9.0. This suggests that long-chain *n*-alkanes (terrestrial plants-derived OC) underwent higher degradation than short-chain *n*-alkanes (OC_{auto}). The $CPI_{25\text{-}33}$ exhibited a decreasing trend from the headwater zone to the estuary in the CRB, indicating a gradual decrease in the degradation of long-chain *n*-alkanes (terrestrial plants-derived OC). In summary, the contribution of phytoplankton to POC increased along the river, while terrestrial plants have the opposite effect. These patterns were closely related to the distribution of terrestrial plants, as well as the interception effect of cascade dams and TGD.

4.2. Source and influencing factors of POC in the CRB

The soil-derived OC was dominant in the CRB, but the contribution of OC_{auto} also played an important role (Fig. 5). The contribution of soil-derived OC showed a decreasing trend from the headwater zone to the estuary (Fig. 5a and b), contrary to the OC_{auto} (Fig. 5d and e). Especially at sampling points below TGD, OC_{auto} showed an increasing trend, indicating the impact of TGD on the composition of POC. The proportion of OC_{auto} increased from TGD to YY, where the C/N value decreased and negative $\delta^{13}C$ values were observed (Fig. 2b and c), indicating an increase in phytoplankton-derived OC. In addition, the OC_{auto} of station YB (located downstream of the Jinshajiang River cascade dams) also increased compared to the stations upstream of the Jinshajiang River. Generally, phytoplankton-derived OC is influenced by weak hydrodynamic conditions. Slower flow rates increase water age and promote the sedimentation of suspended particles, resulting in decreased water turbidity and enhanced photosynthesis of phytoplankton. This explains the increased proportion of OC_{auto} (Liu et al., 2018). Short-chain *n*-alkanes exhibited significant advantages and a high degree of degradation in the the middle and lower reaches CJR (Table 2). This may be attributed to improved transparency caused by sediment interception by the TGD in the upper reach CJR (Tian et al., 2021; Panwar and Yang, 2022; Wang et al., 2022b). Specifically, OC_{auto} dominated in rivers flows into Dongting Lake and Poyang Lake. Where the transparency in the west Dongting lake increased by 45 % from 1996 to 2014 (Tian et al., 2021). The prosperity of algae in the middle and lower reaches CJR (Zhang et al., 2023) aligned with the high contribution of OC_{auto} observed in our study. There was no significant trend in the variation of terrestrial plants-derived OC in the mainstem (Fig. 5c). However, it was significantly higher than other tributaries in the Yalongjiang River, Daduhe River, Minjiang River, and Dongting Lake (Fig. 5d). This could be attributed to differences in vegetation coverage in the river basin. The land-use type map (Fig. 1b) indicated denser grassland and woodland in this region compared to other area. The influence of vegetation cover was reflected in the distribution of long-chain *n*-alkanes ($r = 0.334$, $p < 0.05$; Table S4, Supplementary Material). Surface runoff transported leaf litter from riparian zones as well as leaves and wood debris eroded from the soil into the river. The $\delta^{13}C$ values reflected the carbon fixation pathway of photosynthesis in different organisms, such as C_3 and C_4 plants (Onstad et al., 2000). It has been reported that the average $\delta^{13}C$ values of C_3 plants and C_4 plants were -28.2 ‰ ± 1.9 ‰ and -12.6 ‰ ± 0.3 ‰, respectively (Yu et al., 2007). Given that the decrease in $\delta^{13}C$ value from − 23.74 ‰ to − 29.22 ‰, C_3 plants dominated the CRB (Wu et al., 2007a). Furthermore, the lignin phenol composition in the headwater zone and the Jinshajiang River primarily indicated the woody gymnosperm tissue, while the non-woody angiosperm tissue dominated in the middle and lower reaches CJR.

4.3. Variation of POC under the influence of human activities

We compared the POC contents of the research samples using the same sample method during the flood season in 1997, 2003, 2007, 2010, and 2018 with our study (Wu et al., 2001, 2018; Yu et al., 2011; Mao et al., 2011; Wang et al., 2022a,b). Our investigation revealed significant changes in the POC content within the Jinshajiang River, headwater zone and upper reach CJR (Fig. 6). Notably, the POC content of the samples collected from the headwater zone to the Jinshajiang River in 2007 (mean 0.65 % ± 0.14 %) was higher compared to that of 2021 (mean 0.30 % ± 0.09 %). This indicates a decline in POC levels over time. Since our study did not include TSM data, we found through literature review that the TSM concentration at PZH station in 2021 (15.4 mg/L, Lyu et al., 2023) was significantly lower than in 2007 (450.3 mg/L, Mao et al., 2011). Several studies have reported that cultivation activities contribute to the loss of soil-derived OC into water bodies (Batjes and Sombroek, 1997; Guo et al., 2015). This is because mechanical clearing and tillage may further cause the removal of topsoil and disrupt soil aggregates (Ashagrie et al., 2007), whereby making soil OC more likely to enter water bodies with rainfall. It is worth noting that the cultivated land area has decreased by 342 km^2 from 2005 to 2020, which makes large-grained soil with low POC less susceptible to erosion. Consequently, cultivation can be identified as one of the factors affecting the POC content from the headwater zone to the Jinshajiang River. Furthermore, there has been a significant increase in the construction of large cascade dams along the Jinshajiang River over the past few decades (Fig. 1a). These dams have intensified sediment capture from the headwater zone (Yang et al., 2018; Wang et al., 2022b). Wang et al. (2022b) also reported that the presence of these dams led to a significant reduction POC flux by 80–88 % in the Jinshajiang River. The dams reduced the velocity of water body in Jinsha River and increases the retention time of water body, which is conducive to the settlement of suspended matter and the photosynthesis of phytoplankton. However, the density of phytoplankton in the Jinsha River is the lowest in the Changjiang River Basin (Zhang et al., 2023), so the OC_{auto} is not the main factor affecting the POC content. In conclusion, our research demonstrates that the POC content in the Jinshajiang River has experienced significant changes over time, with decreased levels in recent years. The decrease can be attributed to multiple factors, including cultivation activities and the construction of large cascade dams that influence sediment capture and organic carbon transport in the region. In addition, it can be seen that the POC contents in the middle and lower

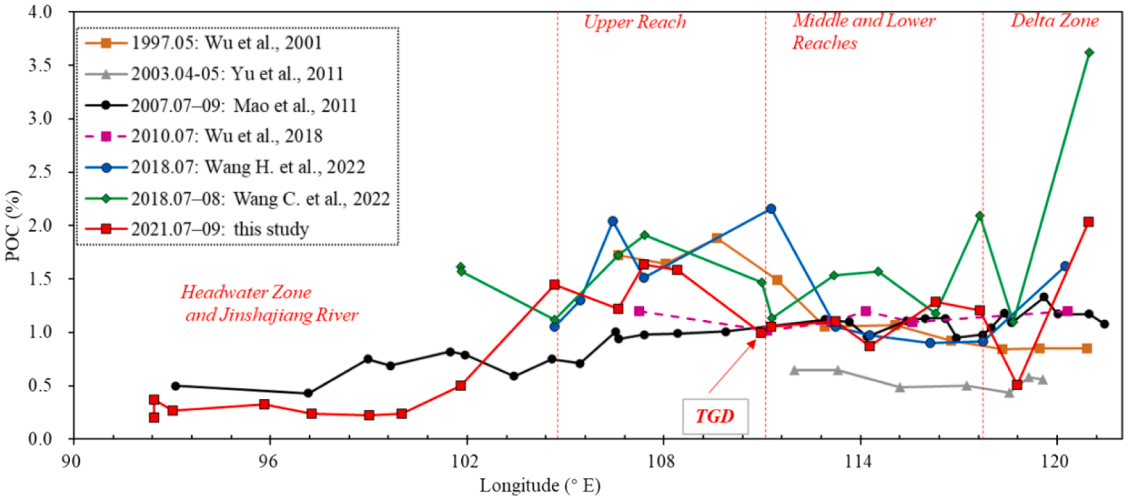

Fig. 6. POC content for POC in mainstem of the CJR from 1997 to 2021.

reaches of the CJR were significantly higher in 1997 than those in 2003 (Wu et al., 2001; Yu et al., 2011), during to TGD intercepting a large amount of sediment in the river channel since 2003 (Yu et al., 2011; Wang et al., 2020a). Between 2007 and 2021, the POC contents recovered to be higher than those in 1997 (Wu et al., 2001, 2018; Mao et al., 2011; Wang et al., 2022a,b), due to an increase in autochthonous OC in water bodies (Bao et al., 2014; Wu et al., 2018).

Numerous studies have previously identified soil-derived OC or OC_{auto} as the primary component of POC in rivers worldwide (Onstad et al., 2000; McCallister et al., 2006; Bao et al., 2014; Marín-Spiotta et al., 2014). However, our study reveals a different scenario in the CRB. We found that both soil-derived and OC_{auto} jointly dominated the POC in the middle and lower reaches as well as the delta zone of the CRB, contrasting with earlier research in the region (Wu et al., 2007b; Yu et al., 2011; Wang et al., 2012). Specifically, the contribution of soil-derived OC proportion was higher in 2010 (44–56 %) (Bao et al., 2014; Wu et al., 2018) compared to 2021 (38–53 %) in the samples collected from the mainstem, spanning from the middle and lower reaches to the estuary. This decline in soil-derived OC can be attributed to two factors: the reduction in cultivated land area and soil erosion area. Over time, the cultivated land area in the CRB decreased from 501,958 km^2 in 1990 to 477,098 km^2 in 2020, and the total area affected by soil erosion also continuously decreased from 530,800 km^2 in 1997 to 337,000 km^2 in 2020, as reported by the Bulletin of Soil and Water Conservation (CWRCMWR, 2005, 2006-2015, 2018, 2020) in the CRB (Figure S2, Supplementary Material). Furthermore, we conducted a comparison of lignin phenols in different years (2003, 2006, 2008, and 2021) and observed higher contents of lignin phenols in the upper reach CJR compared to the middle and lower reaches. Although both Λ8 and Σ8 contents were higher in 2003 than in 2006 and 2021 (Fig. 7a and b), the (Ad/Al)v values exhibited an opposite trend (Fig. 7c). This indicated a decrease in the freshness of lignin phenols over time. Additionally, we analyzed the concentration of *n*-alkanes in the CRB from 1997 to 2021 (Fig. S3a, Supplementary Material). In 1997, the concentration of n-C_{14-33} alkanes increased along the mainstem and was significantly higher than the values observed in 2021 (Fig. S3a, Supplementary Material). The proportions of n-C_{21} + n-C_{23} + n-C_{25} *n*-alkanes ($c(ALK_{mac})$) were lower in 2021 than in 2003 (Fig. S3c, Supplementary Material), whereas the proportions of n-C_{15} + n-C_{17} + n-C_{19} ($c(ALK_{phy})$) *n*-alkanes were opposite (Fig. S3d, Supplementary Material). This suggested a decrease in terrestrial plant-derived OC and a rise in phytoplankton-derived OC. Additionally, both CPI_{14-22} and CPI_{25-33} showed higher values in 2021, followed by 1997 and 2003 (Qi, 2006; Wu et al., 2007a. Fig. S3e and f, Supplementary Material), indicating an upswing in the degradation of *n*-alkanes. This expansion may be caused by the slowing down of water flow during TGD operation, which raised the retention time of water bodies (lignin phenols and *n*-alkanes) (Yu et al., 2011; Wang et al., 2022a). Moreover, nitrogen and phosphorus are crucial nutrients for phytoplankton growth. Generally, and increased concentrations of these nutrients in water can lead to phytoplankton blooms (Zhang et al., 2023). Long-term observations by Ge et al. (2020) also revealed an upward trend in dissolved inorganic nitrogen and phosphorus concentrations from 1999 to 2017 at Datong station. However, the shrinking of a large number of macrophytes in reservoirs and lakes, which have poor connectivity between rivers and lakes, has resulted in a dominance of phytoplankton over macrophytes as the primary source of OC (Tang, 2020). Therefore, the increase in nitrogen and phosphorus nutrients is a significant factor leading to the rise of OC_{auto}.

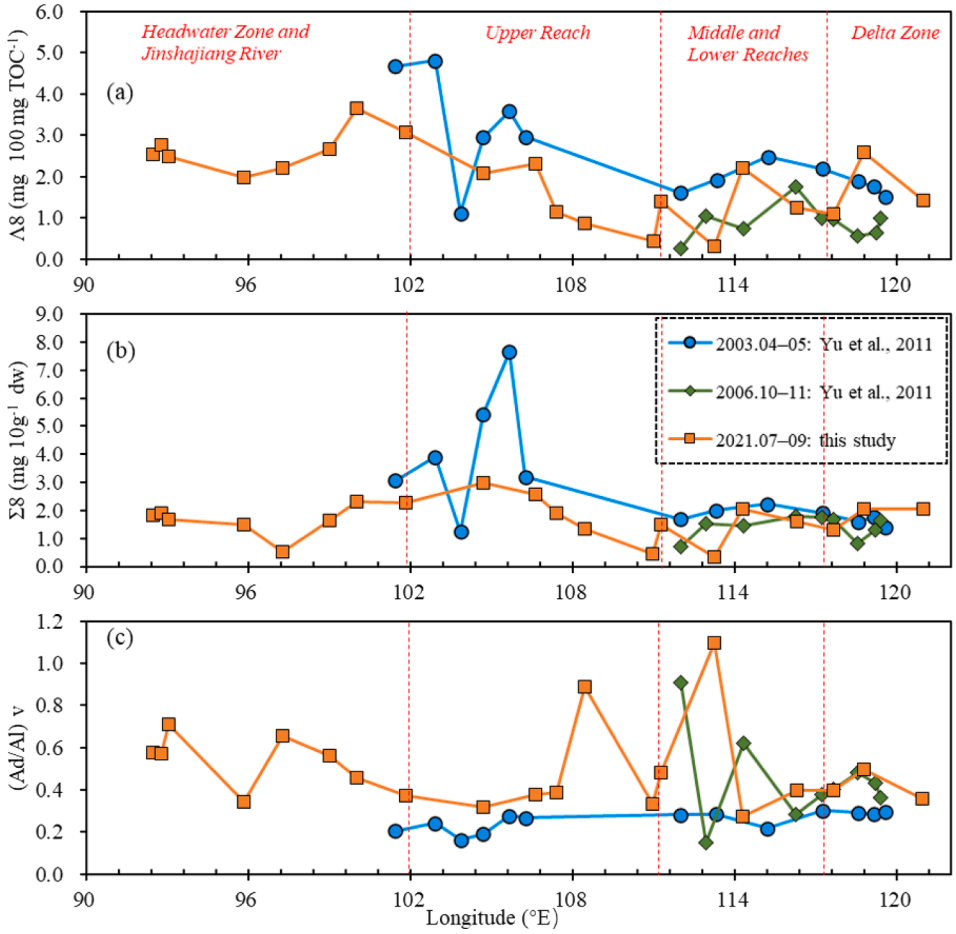

Fig. 7. Distribution patterns of lignin phenol parameters in mainstem of the CJR from 2003 to 2021: (a) Λ8 contents, (b) Σ8 contents, and (c) (Ad/Al)v.

5. Conclusions

In this study, we conducted an analysis of bulk POC properties and biomarkers in the CRB during the rainy season of 2021. Notably, we observed that the POC content exhibited a pattern of variation along the mainstem. Specifically, the POC content was found to be lowest in the headwater zone and Jinshajiang River, while it gradually increased from the headwater zone towards the estuary. Additionally, we noted higher POC contents in the tributaries of the middle and lower reaches CJR compared to the upper reach CJR. Interestingly, the lignin phenol and *n*-alkanes contents displayed a contrary trend to the POC contents, gradually decreasing along the mainstem from the headwater zone. Through a three-end-member mixing model, we were able to estimate the contributions of different sources of OC in the CRB. Soil-derived OC and OC_{auto} accounted for varying percentages in the CRB, ranging from 26.5 % to 60.0 % and 28.1 % to 61.3 %, respectively, with average values of 48.4 % ± 6.8 % and 40.1 % ± 6.7 %. Above the TGD, the soil-derived OC was higher than OC_{auto}. While the proportion of OC_{auto} increased from TGD to estuary, and even higher than soil-derived OC at station YY and DT, due to sediment trapping caused by the TGD. The contributions of terrestrial plants were estimated to be 11.8 % ± 2.0 %. Furthermore, we observed a decline in POC content from 2007 to 2021 at sampling points in the Jinshajiang River and headwater zone. This reduction can be attributed to two factors: the decrease in cultivated land area and the sediment trapping effect of cascade dams. The operation of the TGD resulted in an increased retention time of terrestrial plants debris in the water, leading to an escalated degradation degree of lignin phenols and *n*-alkanes from the upper reach CJR to the estuary. Given these findings, it is essential to conduct further research to understand the implications of reduced soil-derived OC and increased OC_{auto} in CRB on the OC burial in the ECS. Such investigations will help us gain a comprehensive understanding of the complex dynamics of OC in this vital region.

Formatting of funding sources

The work was supported by the Natural Science Foundation of China (Grant No. 42106056); the Marine Science and Technology Innovation Project of Jiangsu Province (Grant No. JSZRHYKJ202206); the Fundamental Research Funds for the Central Universities (Grant No. 0209–14370407); the China Postdoctoral Science Foundation (Grant No. 2021 M691504); and the CRSRI Open Research Program (Grant No. CKWV2021895/KY).

CRediT authorship contribution statement

Yameng Wang: Writing – review & editing, Writing – original draft, Visualization, Software, Project administration, Methodology, Investigation, Formal analysis, Data curation. **Chenglong Wang:** Writing – review & editing, Project administration, Funding acquisition, Conceptualization. **Chuchu Zhang:** Software, Investigation. **Qihang Liao:** Investigation. **Ziyue Feng:** Software. **Xinqing Zou:** Writing – review & editing, Project administration, Funding acquisition, Conceptualization.

Declaration of competing interest

The authors declare that they have no known competing financial interests or personal relationships that could have appeared to influence the work reported in this paper.

Data availability

Data will be made available on request.

Appendix A. Supplementary data

Supplementary data to this article can be found online at https://doi.org/10.1016/j.catena.2024.108083.

References

Andersson, A., 2011. A systematic examination of a random sampling strategy for source apportionment calculations. SCI. Total Environ. 412–413, 232–238. https://doi.org/10.1016/j.scitotenv.2011.10.031.

Ashagrie, Y., Zech, W., Guggenberger, G., Mamo, T., 2007. Soil aggregation, and total and particulate organic matter following conversion of native forests to continuous cultivation in Ethiopia. Soil till. Res. 94 (1), 101–108. https://doi.org/10.1016/j.still.2006.07.005.

Bao, H.Y., Wu, Y., Zhang, J., Deng, B., He, Q., 2014. Composition and flux of suspended organic matter in the middle and lower reaches of the Changjiang (Yangtze River) - impact of the Three Gorges Dam and the role of tributaries and channel erosion. Hydrol. Process. 28 (3), 1137–1147. https://doi.org/10.1002/hyp.9651.

Batjes, N.H., Sombroek, W.G., 1997. Possibilities for carbon sequestration in tropical and subtropical soils. Global Change Biol. 3, 161–173. https://doi.org/10.1046/j.1365-2486.1997.00062.x.

Bourbonniere, R.A., Meyers, P.A., 1996. Sedimentary geolipid records of historical changes in the watersheds and productivities of lakes Ontario and Erie. Limnol. Oceanogr. 41 (2), 352–359. https://doi.org/10.4319/lo.1996.41.2.0352.

Cai, Y.H., Guo, L.D., Wang, X.R., Aiken, G., 2015. Abundance, stable isotopic composition, and export fluxes of DOC, POC, and DIC from the Lower Mississippi River during 2006–2008. J. Geophys. Res. Biogeosci. 120, 2273–2288. https://doi.org/10.1002/2015JG003139.

Canuel, E.A., Hardison, A.K., 2016. Sources, ages, and alteration of organic matter in estuaries. Ann. Rev. Mar. Sci. 8, 409–434. https://doi.org/10.1146/annurev-marine-122414-034058.

Changjiang Water Resources Commission of the Ministry of Water Resources (CWRCMWR)., 2005, 2006–2015, 2018, 2020. Announcement on Water and Soil Conservation in the Changjiang River Basin. Retrieved from http://www.cjw.gov.cn/zwzc/bmgb/stbcgb/.

Changjiang Water Resources Commission of the Ministry of Water Resources (CWRCMWR)., 2016–2021. Changjiang Sediment Bulletin. Retrieved from http://www.cjw.gov.cn/zwzc/bmgb/nsgb/.

Fahl, K., Stein, R., 1997. Modern organic carbon deposition in the Laptev Sea and the adjacent continental slope: Surface water productivity vs. terrigenous input. Org. Geochem. 26(5–6), 379–390. doi: 0.1016/S0146-6380(97)00007-7.

Fearnside, P.M., Pueyo, S., 2012. Greenhouse-gas emissions from tropical dams. Nat. Clim. Change. 2 (6), 382–384. https://doi.org/10.1038/nclimate1540.

Galy, V., France-Lanord, C., Beyssac, O., Faure, P., Kudrass, H., Palhol, F., 2007. Efficient organic carbon burial in the Bengal fan sustained by the Himalayan erosional system. Nature 450 (7168), 407–410. https://doi.org/10.1038/nature06273.

Galy, V., Beyssac, O., France-Lanord, C., Eglinton, T., 2008. Recycling of graphite during Himalayan erosion a geological stabilization of carbon in the crust. Science 322, 943–945. https://doi.org/10.1126/science.1161408.

Galy, V., Peucker-Ehrenbrink, B., Eglinton, T., 2015. Global carbon export from the terrestrial biosphere controlled by erosion. Nature 521, 204–207. https://doi.org/10.1038/nature14400.

Ge, J.Z., Shi, S.Y., Liu, J., Xu, Y., Chen, C.S., Bellerby, R., Ding, P.X., 2020. Interannual variabilities of nutrients and phytoplankton off the changjiang estuary in response to Changing River inputs. J. Geophys. Res- Oceans. 125 (3), 1–23. https://doi.org/10.1029/2019JC015595.

Goñi, M.A., Nelson, B., Blanchette, R.A., Hedges, J.I., 1993. Fungal degradation of wood lignins: Geochemical perspectives from CuO-derived phenolic dimers and monomers. Geochim. Cosmochim. Ac. 57, 3985–4002. https://doi.org/10.1016/0016-7037(93)90348-Z.

Guo, J.J., 2015. Changes of soil carbon pool in typical areas of Changjiang drainage basin and Carbon sequestration potential. China University of Geosciences, Beijing. Master thesis.

Guo, L.C., Su, N., Townend, I., Wang, Z.B., Zhu, C., Wang, X.Y., Zhang, Y.N., 2019. From the headwater to the delta: A synthesis of the basin-scale sediment load regime in the Changjiang River. Earth-Sci. Rev. 197, 1–19. https://doi.org/10.1016/j.earscirev.2019.102900.

Guo, J.J., Xia, X.Q., Yang, Z.F., Yu, T., Hou, Q.Y., 2015. Changes of soil carbon pool in typical areas of Changjiang drainage basin and its influencing factors. Earth Science Frontiers 6 (22), 241–250. https://doi.org/10.13745/j.esf.2015.06.020.

He, H., Liu, Z., Chen, C., Wei, Y., Bao, Q., Sun, H., Yan, H., 2020. The sensitivity of the carbon sink by coupled carbonate weathering to climate and land-use changes: Sediment records of the biological carbon pump effect in Fuxian Lake, Yunnan, China, during the past century. Sci. Total Environment. 720, 137539 https://doi.org/10.1016/j.scitotenv.2020.137539.

Hedges, J.I., Clark, W.A., Cowie, G.L., 1988. Organic matter sources to the water column and surficial sediments of a marine bay. Limnol. Oceanogr. 33, 1116–1136. https://doi.org/10.4319/lo.1988.33.5.1116.

Hedges, J.I., Mann, D.C., 1979. The characterization of plant tissues by their lignin oxidation products. Geochim. Cosmochim. Ac. 43 (11), 1803–1807. https://doi.org/10.1016/0016-7037(79)90028-0.

Hilton, R.G., 2017. Climate regulates the erosional carbon export from the terrestrial biosphere. Geomorphology. 277, 118–132. doi: j. geomorph.2016.03.028.

Hu, Y.X., Gao, L., Qu, R.C., Huang, J., Hu, S., Zhou, Z., Wang, Y.C., Zhang, J., 2022. Community composition and assessment of the aquatic ecosystem of periphytic algae in the Yangtze River basin. Environmental Science 43 (8), 3998–4007. https://doi.org/10.13227/j.hjkx.202111229.

Hu, B.Q., Li, J., Bi, N.S., Wang, H.J., Wei, H.L., Zhao, J.T., Xie, L.H., Zou, L., Cui, R.Y., Li, S., Liu, M., Li, G.G., 2015. Effect of human-controlled hydrological regime on the source, transport, and flux of particulate organic carbon from the lower Huanghe (Yellow River). Earth Surf. Process. Landforms. 40, 1029–1042. https://doi.org/10.1002/esp.3702.

Jiang, X.Z., Lu, B., He, Y.H., 2013. Response of the turbidity maximum zone to fluctuations in sediment discharge from river to estuary in the Changjiang Estuary (China). Estuar. Coast. Shelf s. 131, 24–30. https://doi.org/10.1016/j.ecss.2013.07.003.

Kendall, C., Silva, S.R., Kelly, V.J., 2001. Carbon and nitrogen isotopic compositions of particulate organic matter in four large river systems across the United States. Hydrol. Process. 15 (7), 1301–1346. https://doi.org/10.1002/hyp.216.

Kirkels, F.M.S.A., Zwart, H.M., Usman, M.O., Hou, S., Ponton, C., Giosan, L., Eglinton, T., Peterse, F., 2022. From soil to sea: sources and transport of organic carbon traced by tetraether lipids in the monsoonal Godavari River. India. BIOGEOSCIENCES. 19, 3979–4010. https://doi.org/10.5194/bg-19-3979-2022.

Le, T.P.Q., Dao, V.N., Rochelle-Newall, E., Garnier, J., Lu, X.X., Billen, G., Duong, T.T., Ho, C.T., Etcheber, H., Nguyen, T.M.H., Nguyen, T.B.N., Nguyen, B.T., Le, N.D., Pham, Q.L., 2017. Total organic carbon fluxes of the Red River system (Vietnam). Earth Surf. Process. Landforms. 42, 1329–1341. https://doi.org/10.1002/esp.4107.

Liu, J., Du, J., Wu, Y., Liu, S., 2018. Nutrient input through submarine groundwater discharge in two major Chinese estuaries: the pearl river estuary and the Changjiang River Estuary. Estuar. Coast. Shelf s. 203, 17–28. https://doi.org/10.1016/j.ecss.2018.02.005.

Lyu, J.X., Shi, Y., Zhang, S., Liu, S.J., Liu, T., Xu, X.M., Yang, G., Gao, J.H., 2023. The reservoirs gradually changed the distribution, source, and flux of particulate organic carbon within the Changjiang River catchment. J. Hydrol. 623, 129808 https://doi.org/10.1016/j.jhydrol.2023.129808.

Mannino, A., Harvey, H.R., 1999. Lipid composition in particulate and dissolved organic matter in the Delaware Estuary: Sources and diagenetic patterns. Geochim. Cosmochim. Ac. 63, 2219–2235. https://doi.org/10.1016/S0016-7037(99)00128-3.

Mao, C.P., Ji, J.F., Yun, L., Yuan, X.Y., Yang, Z.F., Song, Y.X., Chen, J., 2011. Seasonal variation in the flux and isotopic composition of particulate organic carbon along the mainstream of the Changjiang river. Earth Science Frontiers, 18(6), 161–168. Retrieved from https://www.earthsciencefrontiers.net.cn/CN/Y2011/V18/I6/161.

Marín-Spiotta, E., Gruley, K.E., Crawford, J., Atkinson, E.E., Miesel, J.R., Greene, S., Cardona-Correa, C., Spencer, R.G.M., 2014. Paradigm shifts in soil organic matter research affect interpretations of aquatic carbon cycling: transcending disciplinary and ecosystem boundaries. Biogeochemistry. 117 (2–3), 279–297. https://doi.org/10.1007/s10533-013-9949-7.

McCallister, S.L., Bauer, J.E., Ducklow, H.W., Canuel, E.A., 2006. Sources of estuarine dissolved and particulate organic matter: A multi-tracer approach. Org. Geochem. 37 (4), 454–468. https://doi.org/10.1016/j.orggeochem.2005.12.005.

Meyers, P.A., 1997. Organic geochemical proxies of paleoceanographic, paleolimnologic, and paleoclimatic processes. Org. Geochem. 27, 213–250. https://doi.org/10.1016/S0146-6380(97)00049-1.

Meyers, P.A., 2003. Applications of organic geochemistry to paleolimnological reconstructions a summary of examples from the Laurentian Great Lakes. Org. Geochem. 34, 261–289. https://doi.org/10.1016/S0146-6380(02)00168-7.

Ogura, K., Machihara, T., Takada, H., 1990. Diagenesis of biomarkers in Biwa lake sediments over 1 million years. Org. Geochem. 16 (4–6), 805–813. https://doi.org/10.1016/0146-6380(90)90119-K.

Onstad, G.D., Canfield, D.E., Quay, P.D., Hedges, J.I., 2000. Sources of particulate organic matter in rivers from the continental USA: lignin phenol and stable carbon isotope compositions. Geochim. Cosmochim. Ac. 64 (20), 3539–3546. https://doi.org/10.1016/S0016-7037(00)00451-8.

Panwar, S., Yang, S., 2022. Influence of Three Gorges Dam and drought on particulate organic carbon flux and its source in the lower Yangtze River. Biogeochemistry. 158 (2), 269–284. https://doi.org/10.1007/s10533-022-00889-w.

Park, J.H., Nayna, O.K., Begum, M.S., Chea, E., Hartmann, J., Keil, R.G., Kumar, S., Lu, X.X., Ran, L.S., Richey, J.E., Sarma, V.V.S.S., Tareq, S.M., Xuan, D.T., Yu, R.H., 2018. Reviews and syntheses: Anthropogenic perturbations to carbon fluxes in Asian river systems-concepts, emerging trends, and research challenges. Biogeosciences. 15 (9), 3049–3069. https://doi.org/10.5194/bg-15-3049-2018.

Peterson, B.J., Howarth, R.W., Garrett, R.H., 1985. Multiple stable isotopes used to trace the flow of organic matter in estuarine food webs. Science 227, 1361–1363. https://doi.org/10.1126/science.227.4692.1361.

Qi, Y.P., 2006. Distribution of Particulate and Dissolved *n*-Alkanes in the Changjiang and its Adjacent Sea. East China Normal University, Shanghai. Master thesis.

Rao, Z.G., Jia, G.D., Qiang, M.R., Zhao, Y., 2014. Assessment of the difference between mid- and long chain compound specific $\delta D_{n\text{-alkanes}}$ values in lacustrine sediments as a paleoclimatic indicator. Org. Geochem. 76, 104–117. https://doi.org/10.1016/j.orggeochem.2014.07.015.

Rieley, G., Collier, R., Jones, D., Eglinton, G., 1991. The biogeochemistry of Ellesmere Lake, UK. —I: Source correlation of leaf wax inputs to the sedimentary lipid record. Org. Geochem. 17 (6), 901–912. https://doi.org/10.1016/0146-6380(91)90031-E.

Sun, X., Fan, D., Cheng, P., Hu, L., Sun, X., Guo, Z., Yang, Z., 2021. Source, transport and fate of terrestrial organic carbon from Yangtze River during a large flood event: Insights from multiple-isotopes (δ13C, δ15N, Δ14C) and geochemical tracers. Geochim. Cosmochim. Acta 308, 217–236. https://doi.org/10.1016/j.gca.2021.06.004.

Tang, X.Q., 2020. Evolution, driving mechanism and control strategy for eutrophication in Changjiang River Basin. Retrieved from Yangtze River 51 (1), 80–87. http://www.rmcjzz.com/CN/10.16232/j.cnki.1001-4179.2020.01.013.

Tian, Z.B., Wang, L.J., Li, Y.J., Zheng, B.H., Chu, Z.S., 2021. Changes of phosphorus delivery from Yangtze River to Dongting Lake under new water and sediment conditions. J. Clean. Prod. 316, 128248 https://doi.org/10.1016/j.jclepro.2021.128248.

Voss, B.M., Wickland, K.P., Aiken, G.R., Striegl, R.G., 2017. Biological and land use controls on the isotopic composition of aquatic carbon in the Upper Mississippi River Basin. Global Biogeochem. Cycles 31, 1271. https://doi.org/10.1002/2017GB005699.

Wang, X.C., Ma, H.Q., Li, R. H., Song, Z.S., Wu, J.P., 2012. Seasonal fluxes and source variation of organic carbon transported by two major Chinese Rivers: The Yellow River and Changjiang (Yangtze) River. Global Biogeochem. Cy. 26(2), GB2025. doi: 10.1029/2011GB004130, 2012.

Wang, C.L., Hao, Z., Gao, J.H., Feng, Z.Y., Ding, Y.C., Zhang, C.C., Zou, X.Q., 2020a. Reservoir Construction Has Reduced Organic Carbon Deposition in the East China Sea by Half Since 2006. Geophys. Res. Lett. 47, 1–10. https://doi.org/10.1029/2020GL087357.

Wang, Z.C., Mao, H.T., Shen, J.W., Tang, X., Chen, X., 2020b. Analysis of water and sediment characteristics in the main tributaries of the Yangtze River and their associated influence factors. Journal of East China Normal University (natural Science) 1, 126–138. https://doi.org/10.3969/j.issn.1000-5641.201841031.

Wang, H., Ran, X.B., Bouwman, A.F., Wang, J.J., Xu, B.C., Song, Z.L., Sun, S.B., Yao, Q.Z., Yu, Z.G., 2022b. Damming alters the particulate organic carbon sources, burial, export and estuarine biogeochemistry of rivers. J. Hydrol. 607, 127525 https://doi.org/10.1016/j.jhydrol.2022.127525.

Wang, H.J., Saito, Y., Zhang, Y., Bi, N.S., Sun, X.X., Yang, Z.S., 2011a. Recent changes of sediment flux to the western Pacific Ocean from major rivers in East and Southeast Asia. Earth-Sci. Rev. 108 (1–2), 80–100. https://doi.org/10.1016/j.earscirev.2011.06.003.

Wang, M., Zhang, J.L., Gui, Z.S., 2011b. Spatial and Temporal Transport of Organic Carbon in Changjiang Mainstream and Influence of Three Gorges Project. Periodical of Ocean University of China 41 (1/2), 117–124. https://doi: 10.16441/j.cnki.hdxb.2011.z1.018.

Wang, C.L., Zhang, C.C., Wang, Y.M., Jia, G.D., Wang, Y.P., Zhu, C., Yu, Q., Zou, X.Q., 2022a. Anthropogenic perturbations to the fate of terrestrial organic matter in a river-dominated marginal sea. Geochim. Cosmochim. Ac. 333, 242–262. https://doi.org/10.1016/j.gca.2022.07.012.

Wei, B., Mollenhauer, G., Hefter, J., Grotheer, H., Jia, G., 2020. Dispersal and aging of terrigenous organic matter in the Pearl River Estuary and the northern South China Sea Shelf. Geochim. Cosmochim. Acta 282, 324–339. https://doi.org/10.1016/j.gca.2020.04.032.

Wu, Y., Jing, Z., Mi, T.Z., Li, B., 2001. Occurrence of n-alkanes and polycyclic aromatic hydrocarbons in the core sediments of the Yellow Sea. Mar. Chemistry. 76 (1–2), 1–15. https://doi.org/10.1016/S0304-4203(01)00040-8.

Wu, Y., Zhang, J., Liu, S.M., Zhang, Z.F., Chen, H.T., Xiong, H., 2007a. Particulate n-alkanes and fatty acids in the Changjiang river system. Retrieved from Acta Oceanol. Sin. 26 (2), 37–48. http://aosocean.com/en/article/id/20070204.

Wu, Y., Zhang, J., Liu, S.M., Zhang, Z.F., Yao, Q.Z., Hong, G.H., 2007b. Sources and distribution of carbon within the Yangtze River system. Estuar. Coast. Shelf s. 71 (1–2), 13–25. https://doi.org/10.1016/j.ecss.2006.08.016.

Wu, Y., Eglinton, T.I., Zhang, J., Montlucon, D.B., 2018. Spatiotemporal variation of the quality, origin, and age of particulate organic matter transported by the Yangtze River (Changjiang). J. Geophys. Res. Biogeo. 123 (9), 2908–2921. https://doi.org/10.1029/2017JG004285.

Xing, L., Zhang, H., Yuan, Z., Sun, Y., Zhao, M., 2011. Terrestrial and marine biomarker estimates of organic matter sources and distributions in surface sediments from the East China Sea shelf. Cont. Shelf Res. 31 (10), 1106–1115. https://doi.org/10.1016/j.csr.2011.04.003.

Xu, X.L., Liu, J.Y., Zhang, S.W., Li, R.D., Yan, C.Z., Wu, S.X., 2023. Chinese Multi-period Land Use Cover Change. Resource and Environment Science and Data Center.

Yamamoto, M., Okino, T., Sugisaki, S., Sakamoto, T., 2008. Late Pleistocene changes in terrestrial biomarkers in sediments from the central Arctic Ocean. Org. Geochem. 39 (6), 754–763. doi: 0.1016/j.orggeochem.2008.04.009.

Yang, S.L., Xu, K.H., Milliman, J.D., Yang, H.F., Wu, C.S., 2015. Decline of Yangtze River water and sediment discharge: Impact from natural and anthropogenic changes. Sci. Rep-UK 5 (1), 12581. https://doi.org/10.1038/srep12581.

Yang, H.F., Yang, S.L., Xu, K.H., Milliman, J.D., Wang, H., Yang, Z., Chen, Z., Zhang, C. Y., 2018. Human impacts on sediment in the Yangtze River: A review and new perspectives. Global Planet. Change. 162, 8–17. https://doi.org/10.1016/j.gloplacha.2018.01.001.

Yu, H., Wu, Y., Zhang, J., Yao, Q.Z., Zhu, Z.Y., 2007. The characteristics of lignin of plant and soil samples in the Yangtze River (Changjiang) Drainage Basin. Acta Scientiae Circumstantiae 5, 817–823. https://doi.org/10.13671/j.hjkxxb.2007.05.019.

Yu, H., Wu, Y., Zhang, J., Deng, B., Zhu, Z.Y., 2011. Impact of extreme drought and the three gorges dam on transport of particulate terrestrial organic carbon in the Changjiang (Yangtze) River. J. Geophys. Res. 116 (F04029), 2011. https://doi.org/10.1029/2011JF002012.

Zhang, J., Hu, Y.X., Hu, S., Huang, J., 2023. Environmental driving factors and assessment on the aquatic ecosystem of periphytic algae of six inflow rivers in Yangtze River basin. Environ. Sci. 4 (44), 2072–2082. https://doi.org/10.13227/j.hjkx.202206095.

Zhao, M., Sun, H., Liu, Z., Bao, Q., Chen, B., Yang, M., Yan, H., Li, D., He, H., Wei, Y., Cai, G., 2022. Organic carbon source tracing and the BCP effect in the Yangtze River and the Yellow River: Insights from hydrochemistry, carbon isotope, and lipid biomarker analyses. Sci. Total Environ. 812, 152429. https://doi.org/10.1016/j.scitotenv.2021.152429.